A comparison of the behavior of cholesterol, 7-dehydrocholesterol and ergosterol in phospholipid membranes

ARTICLE *in* BIOCHIMICA ET BIOPHYSICA ACTA (BBA) - BIOMEMBRANES · MARCH 2012

Impact Factor: 3.84 · DOI: 10.1016/j.bbamem.2012.03.009 · Source: PubMed

2 AUTHORS, INCLUDING:

Changfeng Chen
Kashiv Pharma, LLC
15 PUBLICATIONS **110** CITATIONS

SEE PROFILE

Biochimica et Biophysica Acta 1818 (2012) 1673–1681

Contents lists available at SciVerse ScienceDirect

Biochimica et Biophysica Acta

journal homepage: www.elsevier.com/locate/bbamem

A comparison of the behavior of cholesterol, 7-dehydrocholesterol and ergosterol in phospholipid membranes

Changfeng Chen, Carl P. Tripp *

Laboratory for Surface Science and Technology and Department of Chemistry, University of Maine, Orono, ME 04469, USA

ARTICLE INFO

Article history:
Received 14 November 2011
Received in revised form 7 March 2012
Accepted 13 March 2012
Available online 20 March 2012

Keywords:
ATR-IR
Detergent insolubility
Zeta potential
Sterol structure
Liposome
DPPC and EggPC

ABSTRACT

A molecular description of the effect of incorporation of cholesterol (CHOL), 7-dehydrocholesterol (7DHC) and ergosterol (ERGO) on the structure of DPPC or EggPC liposomes is provided. Data obtained from ATR-IR spectroscopy, detergent solubility and zeta potential measurements show that the insertion of the various sterols alters the packing arrangement of the tails and headgroup of the PC lipids and may lead to lipid domain formation. On a molecular basis, the differences in lipid packing architecture are traced to differences between the ring and tail structure of the three sterols and these differences in structure produce different effects in DPPC liposomes in the gel phase and EggPC liposomes in the fluid phase. Specifically, CHOL has a relatively flat and linear structure and among the three sterols, shows the strongest molecular interactions with DPPC and EggPC lipids. An extra double bond in the fused ring of 7DHC hinders a tightly packing arrangement with DPPC lipids and leads to less domain formation than CHOL whereas 7DHC clearly produces more lipid domain formation in EggPC. ERGO produces similar structural changes to 7DHC in the tail and headgroup region of DPPC. Nevertheless, ERGO incorporation into DPPC liposomes produces more domain formation than 7DHC.

1. Introduction

There have been several studies aimed at understanding the role of sterols such as cholesterol (CHOL), 7-dehydrocholesterol (7DHC) and ergosterol (ERGO) in altering membrane structure and function [1–11]. ERGO is the major component of cellular membranes in lower eukaryotes such as fungi and insects [7] while higher eukaryotes contain CHOL as their major sterol component. Interest in understanding of the role of 7DHC in membrane function can be traced to its connection with the Smith–Lemli–Opitz syndrome (SLOS).

The SLOS is a recessive disease resulting from the mutations in the gene responsible for the synthesis of the enzyme 3β-hydroxy-sterol-Δ^7-reductase, which is responsible for converting 7DHC to CHOL [11,12]. This genetic defect in SLOS leads to a decrease in CHOL and an increase in 7DHC content in membranes [10], and this imbalance is believed to contribute to SLOS pathogenicity. For example, Tulenko et al. [11] showed that an increased level of 7DHC resulted in a 20% increase in the membrane fluidity of skin fibroblasts isolated from normal and SLOS subjects. This change in membrane fluidity produced a three-fold increase in calcium permeability and was accompanied by a marked decrease in the Na/K ATPase activity.

The molecular basis underlying the effects of the three sterols on changing membrane structure is less understood. As shown in Fig. 1, CHOL and 7DHC differ by a single extra double bond between the 7th and 8th carbon atom in 7DHC while ERGO differs from 7DHC by an additional double bond and methyl group in the alkyl chain region of ERGO. There have been few studies which attempt to connect these subtle differences in chemical structure to the dramatic changes in the biological function of the membrane.

Serfis et al. [5] measured the pressure–area isotherms of CHOL and 7DHC impregnated in L-α-phosphatidylcholine (EggPC) monolayer films and found that the onset of a pressure rise for 7DHC occurred at a lower molecular area than CHOL. This showed that an EggPC–7DHC monolayer possesses a slightly larger molecular area than an EggPC–CHOL monolayer. In later work by this group [13] using a combination of fluorescence microscopy with pressure–area isotherms, they found that incorporation of 7DHC into a DPPC film resulted in less domain formation compared to 1,2-dipalmitoyl-sn-glycero-3-phoscholine (DPPC) films produced containing CHOL. It was concluded that the additional double bond in the 7DHC leads to "puckering" of the 7DHC which, in turn, leads to a less tightly packed DPPC monolayer than obtained with CHOL. Xu et al. [2,9] examined the effect of the structure of the sterol such as CHOL, 7DHC and ERGO on the domain formation in liposomes using fluorescence quenching and detergent solubility. They found that 7DHC and ERGO promote the formation of lipid domains more than CHOL in liposomes composed of DPPC/dioleoyl PC. Smondyrev and Berkowitz [14] performed molecular dynamic simulations of the structure of dimyristoylphosphatidylcholine (DMPC) with CHOL, ERGO and lanosterol and found that lanosterol showed some differences in behavior with respect to tilt

* Corresponding author. Tel.: +1 207 581 2253; fax: +1 207 581 2255.
E-mail address: ctripp@maine.edu (C.P. Tripp).

0005-2736/$ – see front matter © 2012 Elsevier B.V. All rights reserved.
doi:10.1016/j.bbamem.2012.03.009

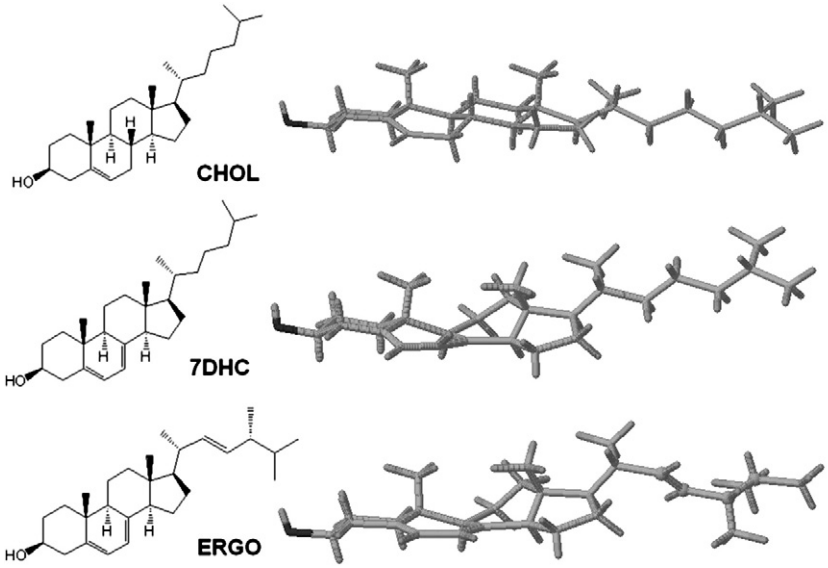

Fig. 1. Chemical structures and 3D conformations of CHOL, 7DHC and ERGO.

angles and degree of hydrogen bonding and this was attributed to a larger size of the first ring of lanosterol. While these studies show that CHOL, 7DHC and ERGO behave differently in terms of membrane packing, the molecular detail of the interactions of these sterols with PC lipids and other lipids is still very incomplete.

Recently, we used ATR-FTIR spectroscopy to study the effect of CHOL level on the fluidity of the membranes in EggPC liposomes [15]. Molecular detail of the interaction of CHOL with the membrane was determined from the changes in IR bands due to the headgroup and the hydrocarbon tail of EggPC with CHOL loading in combination with measurement of release rate of IR probes across the membrane. It was shown that the wavenumber and width of bands assigned to the hydrocarbon tail were sensitive to the packing architecture in the acyl chain region and that a more tightly packed membrane led to a faster release of the IR probe from the liposome.

In this study, we also use the ATR-FTIR method to provide better insight on the molecular interactions of CHOL, 7DHC and ERGO in a simplified membrane system using DPPC and EggPC lipid bilayer membranes. The data obtained from the infrared spectra was combined with the information derived from detergent solubility, and zeta potential measurements. The detergent solubility provided information on domain formation in the membranes [2,8,16,17] and zeta potential of DPPC and EggPC liposomes containing CHOL, 7DHC and ERGO provided information related to conformational changes of the lipid headgoup [18].

2. Materials and methods

2.1. Materials

EggPC (L-α-phosphatidylcholine) and DPPC (1,2-dipalmitoyl-sn-glycero-3-phosphocholine) with a purity >99% from Avanti Polar Lipids (Alabaster, AL) were used without further purification. Cholesterol (CHOL, purity >99%) and 7-dehydrocholesterol (7DHC, >98.5%) were obtained from Sigma-Aldrich and ergosterol (ERGO, >96%) was purchased from Alfa Aesar. Spectrophotometric grade chloroform and methanol were purchased from Fisher Scientific.

2.2. Preparation of liposomes

DPPC and EggPC liposomes with varying amounts of CHOL, 7DHC and ERGO were prepared using a standard method [19]. In brief, a lipidic film was formed by rotary evaporation of a lipid/$CHCl_3$ (200 mg in 6 ml) solution. The film was then hydrated at 10 °C above the main phase transition of the corresponding lipid mixture, 25 °C for EggPC and 50 °C for DPPC. This procedure produced multilamellar lipid vesicles (MLV) which were then divided into two equal samples. One sample was used for detergent insolubility studies, and the second sample was used to prepare small unilamellar vesicles (SUVs). The SUVs were prepared by applying freeze–thaw cycles (5 times) and then followed by extrusion of the sample 20 times through a 100 nm polycarbonate membrane. The freeze–thaw cycles were carried out by immersion of the vial containing the sample in liquid N_2 and then a water bath.

2.3. Zeta potential

The zeta potential of the extruded liposomes diluted to a concentration of about 1 g lipid/l (using 1 mM Tris buffer, pH 7.4) was measured on a Malvern Zetasizer 3000 system. Measurements were performed at 24 ± 1 °C in triplicate on three samples. The size for all 4 types of liposomes was in the range of 100–130 nm and had a narrow size distribution with polydispersity index (PI) values lower than 0.1.

2.4. Liposome solubilization

Solubilization of the liposomes after addition of detergent was monitored by the change in the optical density (OD) of the suspension at 400 nm [9]. The presence of liposomes increases the amount of light scattered by the suspension and hence an increase in the OD. Addition of Triton X-100 leads to solubilization of the liposomes resulting in a decrease in the amount of light scattering and thus a decrease in the OD.

A liposomal suspension containing 500 nmol of total lipids was prepared in a standard 1 cm cuvette by dispersing 50 μl of an 8 mg/ml MLV in 900 μl PBS solution (10 mM sodium phosphate and 150 mM NaCl, pH 7). The OD of the suspension was then measured on a Beckman 650 spectrophotometer. A 50 μl aliquot of a 10% (w/v) Triton X-100/PBS was then added to the cuvette. After initial hand mixing for 1 min, the sample was left to stand for 2 h. The OD of the suspension was then remeasured. Longer incubation time (4 h and 20 h) showed only a slight decrease (<10%) in OD compared to the value measured at 2 h. The OD% was then calculated and was defined as the ratio of the OD after Triton X-100 incubation of 2 h divided by the OD value obtained before addition of the detergent. Thus, a higher %OD value means that

the liposome is more resistant to detergent solubilization. All experiments were carried out at a temperature of 24 ± 1 °C and were performed a minimum of three times.

2.5. IR transmission of the insoluble membrane fraction

Liposomal suspensions were divided into two equal samples. One sample served as the control and Triton X-100 was added to the second sample following the procedure used in measuring %OD. After a 2 h incubation with Triton X-100, the sample and control sample were centrifuged for 15 min at 10,000 RCF in a Beckman Coulter Allegra™ 21R centrifuge. The supernatant was decanted and the remaining solids were washed twice by resuspending in 1 ml deionized water and collected by centrifugation. The solids were dissolved in methanol and then deposited on silicon chips. The chips were allowed to dry overnight in the gentle stream of nitrogen gas to remove residual methanol and water prior to recording an IR spectrum.

The IR transmission spectra were recorded on a ABB FTLA 2000 FTIR spectrometer equipped with a Deuterated Triglycine Sulfate (DTGS) detector and a standard 13 mm pellet holder. Each spectrum consists of 50 co-added scans at a resolution of 8 cm^{-1}. A reference spectrum was recorded through a blank silicon window.

2.6. ATR-FTIR spectroscopy

ATR-FTIR spectra were recorded on a Bomem MB-series FTIR spectrometer equipped with a liquid N_2-cooled mercury cadmium telluride (MCT) detector and fitted with a standard ATR liquid flow cell (Harrick Scientific, Pleasantville, NY, USA). The internal reflection element (IRE) was a ZnSe crystal (50 × 10 × 2 mm) beveled at 45°. Each spectrum consisted of 100 co-added scans at a resolution of 4 cm^{-1}. A reference spectrum was recorded with a clean ZnSe crystal mounted in the liquid flow cell.

The wavenumber position for the symmetric stretching CH_2 mode (~2850 cm^{-1}) and the C═O stretching mode (~1730 cm^{-1}) was determined using a curve fitting program and calculating a second derivative, respectively, using Grams/32 version 7.0 from Galactic Software. Specifically, the peak position of the CH_2 peak was obtained by fitting the region between 3000 and 2800 cm^{-1} to six peaks using a 100% Lorentzian lineshape. For the C═O band, a second derivative curve in the range between 1775 and 1685 cm^{-1} was generated which showed the presence of two bands centered around 1741 cm^{-1} and 1728 cm^{-1}. These two frequencies were chosen for curve fitting the carbonyl band region. During the fitting procedure, the peak position of the high wavenumber component near 1741 cm^{-1} was fixed to a value obtained by calculating the second derivative while the peak position of the 1728 cm^{-1} band was allowed to vary during application of the curve fitting routine as this band was much broader and therefore the peak maxima was difficult to determine. The percent of Lorentzian was fixed at 50% as this leads to best fits as judged by the residual signal.

2.7. Preparation of lipid film on ZnSe IRE

The procedure used for generating a lipid film on a ZnSe IRE is described elsewhere [20]. Specifically, a 300 µl sample of the extruded liposomal suspension at a concentration of 8 mg/ml was pipetted across the entire surface of ZnSe IRE. The IRE was then placed into a humidity chamber filled with dry nitrogen gas. A thin lipid film on the IRE was obtained after slow evaporation of the water overnight. The ZnSe crystal containing the dried lipid film was mounted in a Harrick ATR flow cell and the lipid film was rehydrated by adding 400 µl of a 5 mM $NaHCO_3$ (pH 7.8) solution to the liquid flow cell followed by incubation for 15–20 min.

2.8. Modeling of 3D structures of CHOL, 7DHC and ERGO

PCMODEL 8.0 (Serena Software, Bloomington, IN) was used to model the 3D chemical structures of the three sterols. The structures of CHOL, 7DHC and ERGO showed in Fig. 1 were calculated using MMX3.

3. Results

3.1. Detergent insolubility

Fig. 2A and B shows the %OD (and by inference, detergent solubilization by Triton X-100) of DPPC and EggPC lipids with various mole% of CHOL, 7DHC and ERGO, respectively. As shown in Fig. 2A, the presence of all three sterols increases the insolubility of DPPC liposomes to Triton X-100 and the insolubility for CHOL and ERGO is higher than that for 7DHC at 20 mol% loading. At 40 mol% the presence of CHOL shows the highest level of insolubility to Triton X-100.

The %OD values obtained for CHOL, 7DHC and ERGO in EggPC liposomes (Fig. 2B) are clearly different from that observed in the DPPC liposomes (Fig. 2A). In particular, the EggPC liposomes containing ERGO are fully solubilized in Triton X-100 at loadings up to 20 mol% and at all loadings up to 50 mol% CHOL, whereas 7DHC shows an

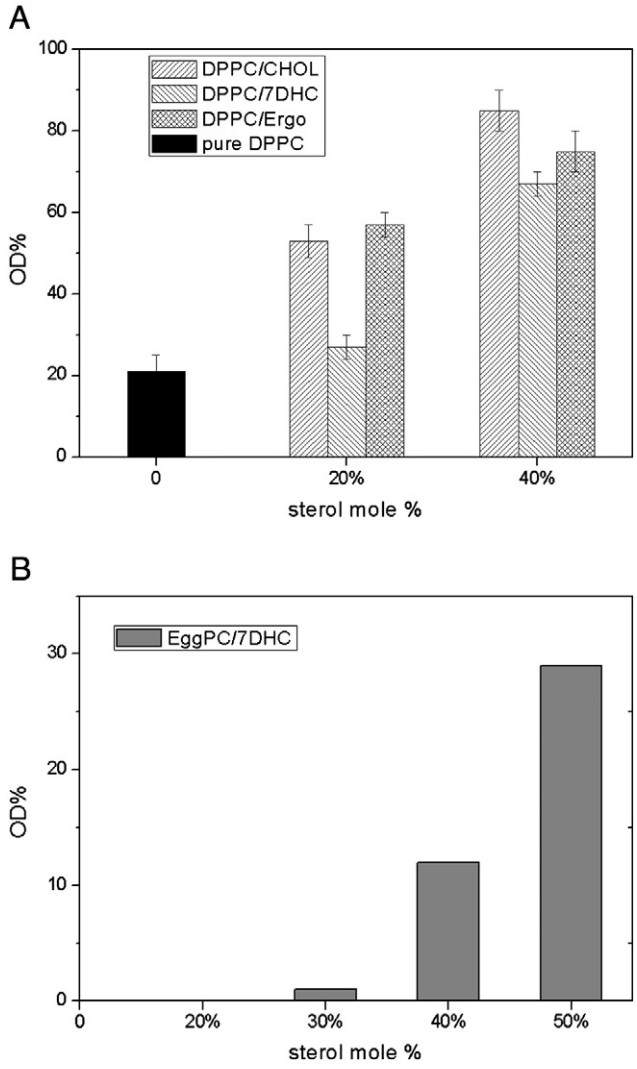

Fig. 2. %OD of lipid mixtures at 23 °C with Triton X-100. (A) DPPC without or with 20 and 40 mol% CHOL, 7DHC and ERGO; (B) EggPC without or with 20, 30, 40 and 50 mol% 7DHC.

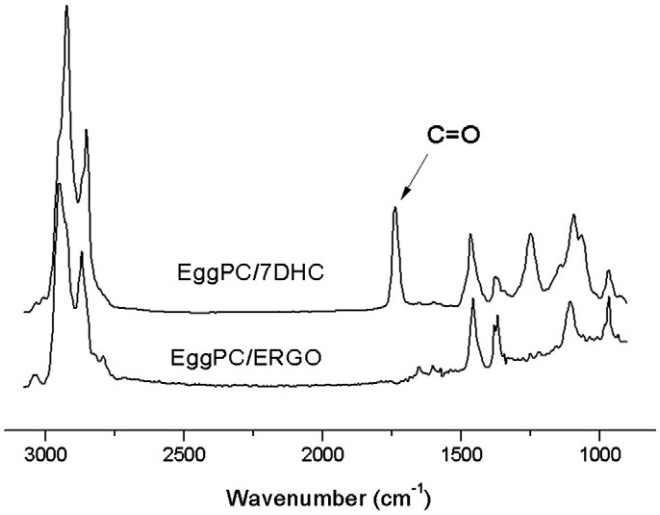

Fig. 3. IR spectra of the detergent insoluble fractions of EggPC/7DHC 50 mol% and EggPC/ERGO 30 mol% liposomes.

increase in insolubility with increasing sterol content. Data for ERGO loaded EggPC above 25 mol% is not presented because this is above the solubility limit for ERGO in EggPC liposomes [7,21,22]. As a result, Fig. 2B shows values only for 7DHC as the other two sterols have values of 0 for %OD. The solubility limit for ERGO in EggPC was confirmed by recording IR spectra of the insoluble fraction of the EggPC/7DHC at 50 mol% and EggPC/ERGO at 30 mol% (see Fig. 3). An intense carbonyl band due to the EggPC lipids in the spectra of 50 mol% EggPC/7DHC shows that the detergent insoluble fraction contains both PC lipids and sterol, whereas this carbonyl band is not present in the spectra with 30 mol% ERGO indicating there are no PC lipids in this fraction. This result shows that the detergent insolubility for ERGO in EggPC liposome depicted in Fig. 2B is due to insoluble ERGO in the aqueous solution and not due to lipid domain formation.

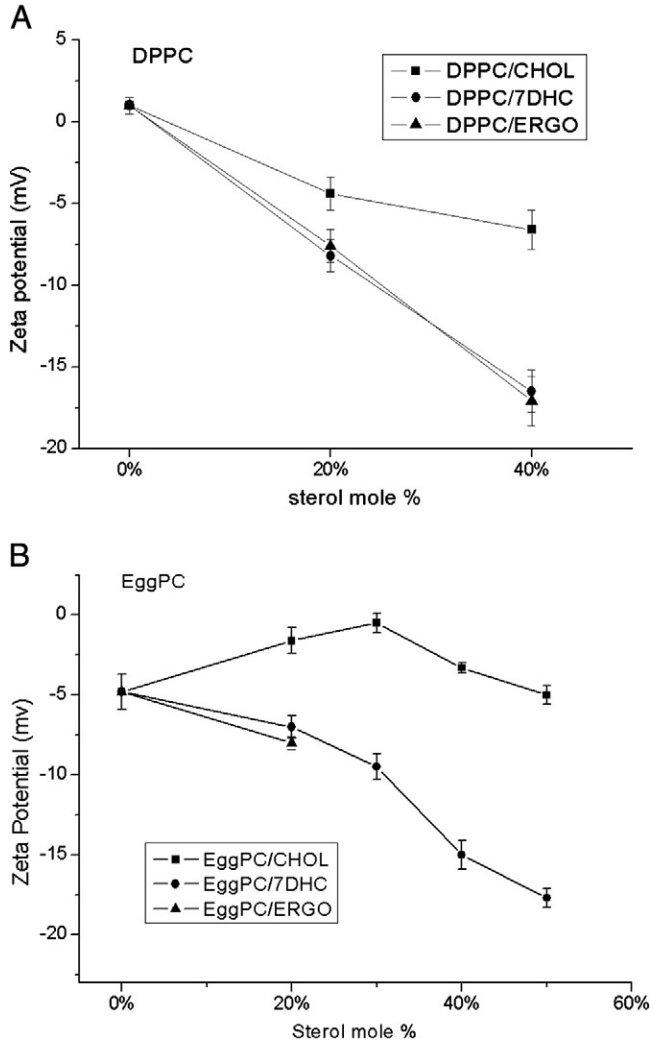

Fig. 4. Zeta potential of unilamellar liposomes. (A) DPPC liposomes without or with 20 and 40 mol% CHOL, 7DHC and ERGO; (B) EggPC liposomes without or with 20, 30, 40 and 50 mol% CHOL, 7DHC and ERGO.

3.2. Zeta potential

Fig. 4A shows that pure DPPC liposome has a slight positive zeta potential and incorporation of sterols in DPPC liposomes results in a decrease in the zeta potential with sterol loading. It is also found that 7DHC and ERGO produce a more negative value in zeta potential than CHOL at a given mole %.

The zeta potential of EggPC with or without sterols is shown in Fig. 4B and is clearly different from the results obtained for DPPC liposomes shown in Fig. 4A. First, while pure DPPC liposomes exhibit a positive zeta potential, pure EggPC liposomes show a negative zeta potential. Secondly, while the zeta potential decreases in value with increased mole% of 7DHC and ERGO, the corresponding zeta potential with CHOL shows little change and even a slight initial increase at 20–30 mol% of CHOL.

3.3. ATR-FTIR

Fig. 5 shows the IR spectra of EggPC, CHOL, 7DHC and ERGO. The wavenumber position of the CH_2 symmetric stretching mode at 2850 cm^{-1} depends on the chain conformational disorder of the hydrocarbon tail of PC molecules and the carbonyl group band at 1730 cm^{-1} is sensitive to the degree of hydration [20,23–25]. Thus a change in the wavenumber of these bands after addition of CHOL, 7DHC and ERGO provides structural details of the lipid bilayer membrane.

As shown in Fig. 5, the spectra of CHOL, 7DHC and ERGO contain bands that overlap with the CH_2 stretching bands (3000–2800 cm^{-1}) of the EggPC. An apparent shift in wavenumber in the CH_2 stretching modes of the DPPC or EggPC due to the presence of these bands was considered. The shift in wavenumber resulting from the bands due to sterols was estimated by subtracting the spectra of pure sterol (accounting for the final wt.% sterol in the liposome) from the spectra of PC–sterol mixtures. It was found that the shift in wavenumber provided by the sterol could be neglected. The largest shift in this subtraction

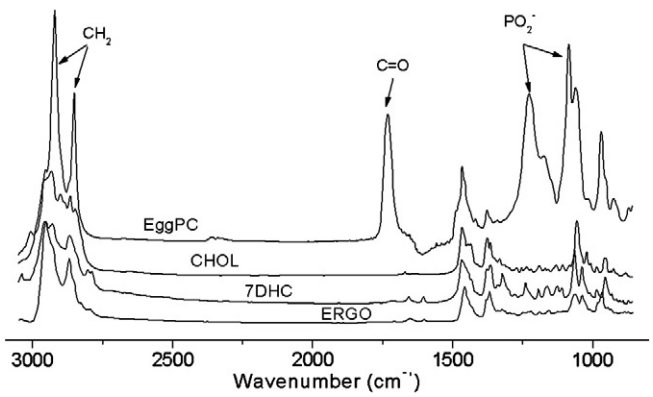

Fig. 5. IR spectra of EggPC, CHOL, 7DHC and ERGO.

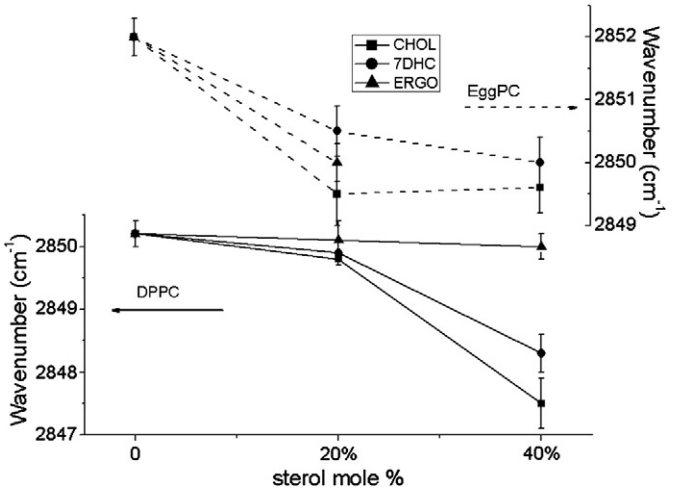

Fig. 6. Wavenumber of CH_2 symmetric stretching mode as a function of increasing mole fraction of CHOL, 7DHC and ERGO in DPPC and EggPC hydrated membranes.

procedure was 0.3 cm^{-1} for 40 mol% CHOL in DPPC or EggPC lipids and this is less than the 1–2 cm^{-1} shift (see Fig. 6) obtained for the CH_2 symmetric stretching mode (2850 cm^{-1}).

Fig. 6 is a plot of the wavenumber position of the CH_2 symmetric stretching mode as a function of CHOL, 7DHC and ERGO mole% in DPPC and EggPC membrane films. In both DPPC and EggPC lipid bilayers, the presence of each sterol results in a shift to lower wavenumber and this shift increases with higher sterol loading. It is also found that the shift in wavenumber is greater with CHOL than 7DHC in both DPPC and EggPC. Insertion of ERGO shows negligible change in the CH_2 band position in DPPC while a larger shift is obtained with ERGO than 7DHC in EggPC liposomes.

The C═O stretching mode is a superposition of two bands with maxima centered near 1741 cm^{-1} and 1727 cm^{-1}. It is known that in hydrated lipid bilayer, the high and low wavenumber C═O stretching modes are attributable to subpopulations of free and hydrogen bonded carbonyl groups (to water or the OH group of the sterol) [20], respectively. Therefore, a higher value in the relative integrated intensity (i.e., ratio of the low wavenumber/high wavenumber C═O band) is reflective of a higher level of hydration in the region close to the ester carbonyl groups of the lipid. In addition, the peak positions and FWHH of the two C═O bands are sensitive to both degree of hydration and conformational change of the lipid bilayer structure [20,23]. The low wavenumber C═O band shifts upward with an increased FWHH and the high wavenumber C═O band shifts upward with a decrease in FWHH for a transition from the gel state to a liquid state for DPPC lipid membrane [20].

Parameters such as peak position, FWHH and relative integrated intensity of the two C═O bands for each type of liposomes are listed in Tables 1 and 2. As shown in Table 1, with increased sterol loading in a DPPC lipid bilayer, there was a shift upward to higher wavenumber and a decrease in the width and relative integrated intensity for the high wavenumber C═O band centered near 1741 cm^{-1}. From our perspective, the relative integrated intensity of the C═O bands is the key parameter to monitor as a change in this value indicates a change in relative population of free and hydrogen bonded C═O groups. Examining the change in the relative integrated intensity of the C═O bands in Table 1, it is found that in all cases, insertion of sterols in the DPPC membranes leads to an increase in the fraction of hydrogen bonded C═O groups. Furthermore, this increase in the fraction of hydrogen bonded C═O groups is greater for 7DHC and ERGO than CHOL at 20 mol% loadings. However, at 40 mol% there is little difference in value for all three sterols.

The changes in the carbonyl stretching modes of EggPC liposomes with sterol loading are given in Table 2 and the trends are opposite from that obtained for DPPC liposomes given in Table 1. In particular, the presence of sterols leads to a shift to lower wavenumber and an increase in FWHH and relative integrated intensity for the high wavenumber component (1741 cm^{-1}).

4. Discussion

4.1. Pure DPPC and EggPC

The detergent insolubility data in Fig. 2 supports the generally accepted picture that, at room temperature, DPPC liposomes are in a gel state where the lipids are tightly packed with the hydrocarbon chain fully extended and EggPC liposomes are in a fluid state in which the hydrocarbon tails are "kinked" and loosely packed [13,26–28]. Specifically, the data in Fig. 2 shows that EggPC liposomes are fully solubilized by Triton X-100 while pure DPPC liposomes are partially solubilized. This is because DPPC is in a tightly packed gel phase and this tighter packing arrangement hinders the penetration of the Triton X-100 surfactant into the membrane.

Zeta potential has been used to evaluate the liposome stability in aqueous solution [29,30] and to investigate molecular changes with the lipid bilayer structure in liposomes [18]. Makino et al. [18] related the change in zeta potential to the conformational changes in the headgroup region of lipid membranes. It was reported that a positive change in zeta potential was indicative of the choline group of the headgroup extending outward from the liposome surface whereas a negative change in value of the zeta potential indicated that the choline group folded inward towards the surface and exposing more of the negatively charged phosphatidyl group to the outer fluid phase (see Scheme 1). Therefore, a more positive zeta potential is normally associated with restricted lipid headgroup movement due to a tight packing between PC lipids, while a more negative zeta potential generally indicates a less tightly packed headgroup region.

The zeta potential values given in Fig. 4 show that pure DPPC liposomes have a slight positive zeta potential while pure EggPC liposomes are negative in value. By analogy to the Makino et al. work, the tightly packed architecture associated with the DPPC liposomes in the gel state forces the choline group to extend outward from the

Table 1
Wavenumber position, FWHH and relative intensity of the C═O band for DPPC liposomes with or without CHOL, 7DHC or ERGO. The relative integrated intensity (Rel. Integr.) for high wavenumber component is calculated by using the integration area of the high wavenumber band divided by the total integration area of the carbonyl band.

	High wavenumber component			Low wavenumber component		
	Peak position (cm^{-1})	FWHH (cm^{-1})	Rel. Integr.	Peak position (cm^{-1})	FWHH (cm^{-1})	Rel. Integr.
DPPC	1739.8 ± 0.2	21.8 ± 0.2	0.47 ± 0.03	1726.0 ± 0.7	24.0 ± 0.5	0.53 ± 0.03
CHOL0.2	1740.5 ± 0.4	21.4 ± 0.8	0.43 ± 0.02	1726.5 ± 0.5	26.9 ± 0.3	0.57 ± 0.02
7DHC0.2	1741.5 ± 0.1	20.0 ± 0.5	0.35 ± 0.04	1727.0 ± 0.5	28.0 ± 1.0	0.65 ± 0.04
ERGO0.2	1741.5 ± 0.2	20.0 ± 0.5	0.35 ± 0.03	1727.0 ± 0.4	29.0 ± 0.5	0.65 ± 0.03
CHOL0.4	1742.5 ± 0.3	18.0 ± 1.0	0.25 ± 0.03	1727.8 ± 0.4	32.0 ± 1.0	0.75 ± 0.03
7DHC0.4	1742.5 ± 0.1	17.0 ± 1.0	0.22 ± 0.05	1727.6 ± 0.6	32.0 ± 2.0	0.78 ± 0.05
ERGO0.4	1742.0 ± 0.2	17.0 ± 0.5	0.25 ± 0.03	1728.0 ± 0.5	32.0 ± 1.0	0.75 ± 0.03

Table 2
Same as Table 1 for EggPC liposomes with or without CHOL, 7DHC or ERGO.

	High-wavenumber component			Low-wavenumber component		
	Peak position (cm^{-1})	FWHH (cm^{-1})	Rel. Integr.	Peak position (cm^{-1})	FWHH (cm^{-1})	Rel. Integr.
EggPC	1741.5 ± 0.4	18.0 ± 0.6	0.15 ± 0.05	1726.0 ± 0.6	32.0 ± 1.0	0.85 ± 0.05
CHOL0.2	1740.6 ± 0.6	19.0 ± 0.4	0.20 ± 0.02	1726.0 ± 0.5	31.0 ± 1.0	0.79 ± 0.02
7DHC0.2	1739.0 ± 0.5	27.0 ± 0.3	0.40 ± 0.03	1723.0 ± 0.6	29.0 ± 1.0	0.60 ± 0.03
ERGO0.2	1741.0 ± 0.2	20.0 ± 0.4	0.25 ± 0.04	1728.0 ± 0.5	31.0 ± 0.5	0.75 ± 0.04
CHOL0.4	1742.0 ± 0.3	21.0 ± 0.2	0.35 ± 0.04	1726.0 ± 0.4	30.0 ± 0.5	0.65 ± 0.04
7DHC0.4	1741.0 ± 0.5	20.0 ± 0.3	0.45 ± 0.03	1725.0 ± 0.6	28.0 ± 0.6	0.55 ± 0.03

liposome surface, thus resulting in a positive zeta potential value. In contrast, EggPC liposomes with a loosely packed hydrocarbon tail mean that the headgroup movement is less restricted and the choline groups tend to fold inward to the liposome center to prevent water penetration to the hydrophobic core. This inward folding of the headgroup exposes the negatively charged phosphatidyl group and results in a negative zeta potential. Thus a larger average molecular surface area for EggPC lipids than DPPC lipids in liposomes can be expected and this is in agreement with those reported average molecular area for EggPC and DPPC lipid (EggPC-62 $Å^2$ [31–33]; DPPC-46 $Å^2$ at 20 °C [34,35]) obtained from X-ray diffraction studies of liposomes.

The IR spectra of the pure DPPC and EggPC lipid membranes support the molecular interpretation derived from the zeta potential data. Fig. 5 shows that the wavenumber position of the CH_2 symmetric stretching mode is located at 2850 cm^{-1} and 2852 cm^{-1} in DPPC and EggPC liposomes, respectively. This shows that the hydrocarbon tails in EggPC liposomes are less tightly packed than in DPPC liposomes [15,25,36].

For the C═O stretching mode, (see Tables 1 and 2) the relative integrated intensity of the low wavenumber component (~1726 cm^{-1}) for DPPC has a value of 53% whereas, this value is 85% for EggPC. This suggests a higher fraction of hydrogen bonded carbonyl groups for EggPC than DPPC. Since there is no sterol present in the pure DPPC and EggPC liposomes, the hydrogen bonding is with water. Penetration of water into the region of the C═O groups would occur more readily in the EggPC membrane given the nature of a more loosely packed lipid bilayer structure compared to the more tightly packed bilayer structure of DPPC liposomes.

4.2. Incorporation of sterols in DPPC and EggPC liposomes

In studying and interpreting the effects of sterols on membrane structure, one must consider the formation of lipid domains. The level of insolubility by Triton X-100 is often correlated with the level of domain formation in PC lipids [2,9,37]. On this basis, the data in Fig. 2A show that CHOL has a stronger ability than 7DHC in promoting domain formation in DPPC lipids. This is in agreement with the results reported by Bering et al. [13]. Using fluorescence microscopy, Berring et al. showed that CHOL forms large isolated domains in a DPPC/CHOL monolayer whereas the incorporation of 7DHC up to 30 mol% showed only a single phase. It was suggested that the ring puckering arising from the extra double bond in the fused ring in 7DHC gives rise to a membrane domain-disrupting effect. However, ERGO also possesses the same distorted ring structure as 7DHC but our data in Fig. 2 shows that ERGO does not lead to the same level of domain disruption as 7DHC. The main difference between 7DHC and ERGO is an extra methyl group in the side chain of ERGO, this leads to an increase in the bulk volume of the side alkyl chain beyond the limits of the sterol body cross section (fused ring region) [4,38]. This may result in a stronger van der Waals interaction between ERGO and the surrounding DPPC lipids in the tail region than with 7DHC and thus rendering the ERGO contained DPPC lipid bilayers more resistant to the attack of surfactant molecules [38].

There have been several studies showing that incorporation of CHOL or other sterols in liposomes composed of unsaturated lipids [e.g., EggPC], are fully solubilized in Triton X-100 [9,17,37]. The result obtained from the detergent solubility in this study with CHOL incorporated in DPPC and EggPC liposomes agrees with these findings. On the other hand, to the best of our knowledge, we are unaware of any detergent insoluble studies with EggPC liposomes containing 7DHC. Clearly, from this work, there is a detergent insoluble fraction formed in 7DHC incorporated EggPC liposomes.

A difference in the lipid compositions of the EggPC/7DHC detergent resistant membrane from the starting EggPC composition is shown by the IR spectra in Fig. 7. The spectrum of EggPC/7DHC 50 mol% and the spectrum of the detergent resistant fraction are normalized to the same amount of PC lipids as indicated by the equal intensity of the band at 1740 cm^{-1} (carbonyl stretching mode). The intensity of the C–H stretching modes (3000–2800 cm^{-1}) is clearly higher in the spectrum of the detergent resistant fraction than in the spectrum obtained for the liposomes before detergent treatment. This difference between these spectra is due to 7DHC indicating a higher content of 7DHC in the detergent resistant fraction. In addition, the band at 3008 cm^{-1} is due to CH_2 band associated with unsaturated group in EggPC lipids and the intensity decrease of this band (relative to the C═O band) in Fig. 7 is indicative of a lower

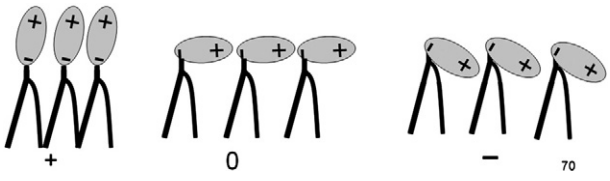

Scheme 1. An illustration of zeta potential change with the headgroup orientation of PC lipids.

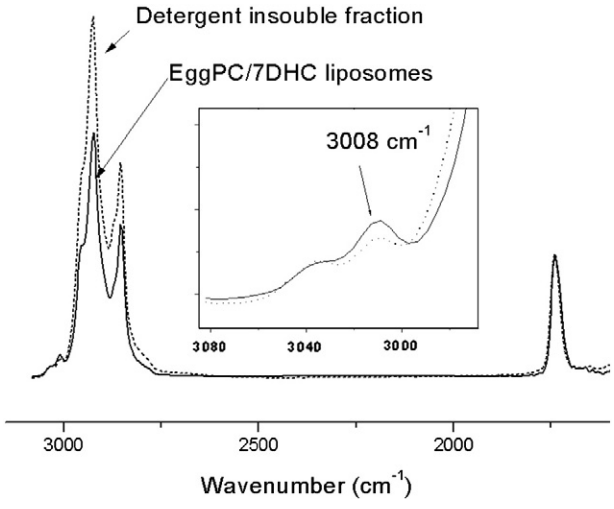

Fig. 7. IR spectra of the EggPC/7DHC 50 mol% liposomes and the detergent insoluble fraction.

percentage of unsaturated PC molecules in the detergent resistant fraction.

EggPC is a mixture of unsaturated lipids (16:0–18:1, 38.2%; 18:0–18:1, 9.3%; 16:0–18:2, 21.8%; 18:0–18:2,11.2%; 18:0–20:4, 3.4%; other 16%) [39]. Therefore, the IR spectra in Fig. 7 show that the detergent resistant fraction consists of the preferential partitioning of the 7DHC into the lipid membrane enriched with lower unsaturated lipids. Specifically, the partitioning of 7DHC occurs preferably in low unsaturated lipids (e.g., PC: 16:0–18:1, 18:0–18:1) and forms detergent resistant domain while those highly unsaturated lipids (e.g., 16:0–18:2, 18:0–18:2, 18:0–20:4) are readily solubilized. This result is supported by other studies in which sterols were generally found to distribute more with saturated or low unsaturated lipids than highly unsaturated lipids [40]. For example, cholesterol distribution into three liposomes prepared with 18:0/18:1 PC, 18:0/18:2 PC and 18:0/20:4 PC was 1: 0.66:0.45, respectively [40].

In DPPC liposomes, the decrease in the zeta potential value is lowest for CHOL while in EggPC there is almost no change in the zeta potential with CHOL. Recall that a larger region for each lipid headgroup to occupy would give rise to a more negative zeta potential of the liposomes. The insertion of sterols in PC lipid bilayers induces two different effects in changing the average area for PC headgroup uptake. First, there is the spacing effect where insertion of cholesterol acts as a "spacer" pushing lipid molecules further apart from each other which, in turn, increases the average area for PC headgroup to occupy. Secondly, incorporation of cholesterol results in a condensing effect [4,41–43] on the surrounding PC lipids which reduces the average molecular area for PC lipids. The spacing and condensing effects would lead to opposite changes in the zeta potential for CHOL incorporation into DPPC and EggPC liposomes.

For DPPC in a gel phase, the PC lipids are tightly packed with an average molecular area around 46 $Å^2$ which is close to the molecular area of CHOL (35 $Å^2$ at 37 °C [5], and 39 $Å^2$ at 22 °C [44]). The condensing effect of cholesterol in the tightly packed DPPC membrane would be small and the spacing effect of cholesterol dominates over the condensing effect leading to an overall increase of the area for DPPC headgroups to occupy. Data from Kim et al. [45] showed that the mean molecular area of a mixed 1:1 DPPC-CHOL monolayer (surface pressure of 20 mN/m; 20 °C) is only 5 $Å^2$ less than the pure DPPC monolayer.

On the other hand, in fluid bilayers (DPPC in liquid phase or EggPC) the lipids are loosely packed and the condensing effect of CHOL does play a role. As shown in Fig. 4, addition of CHOL passes through a maximum in zeta potential at 30 mol% CHOL. This can be explained by the relative contributions of the condensing and spacing effects. With the initial insertion of CHOL in EggPC lipid bilayers, the condensing effect of CHOL dominates over the spacing effect resulting in a decrease of the area for EggPC headgroup to occupy, and thus the zeta potential increases with increasing CHOL content. After about 30 mol% CHOL insertion, the spacing effect of CHOL becomes dominant leading to an overall increase of the area for EggPC headgroup and thus a decrease of the zeta potential of EggPC liposomes.

This is consistent with other studies [31,45] reported that the condensing effect is largest at small cholesterol concentration and saturates at about 30%. For example, Edholm and Nagle [43] determined the average value of area per total lipids versus the molecular fraction of CHOL in a fluid DPPC bilayer (50 °C) [46–48]. It was shown that the average molecular area of lipids in pure DPPC bilayer in the fluid phase was estimated at 65 $Å^2$ and there was a 30 $Å^2$ reduction in the area per lipids in a 1:1 DPPC/CHOL bilayer which is much larger than the 5 $Å^2$ reduction when the same amount of CHOL was incorporated in a DPPC monolayer in gel phase [45].

Fig. 4 also shows that incorporation of 7DHC and ERGO in both DPPC and EggPC liposomes leads to a more negative zeta potential than CHOL at a given sterol mole%. The trend to more negative zeta potential follows the order ERGO = 7DHC > CHOL. This trend can be traced to the chemical structure of each sterol which leads to different levels of contribution by the spacing and condensing effects. Demel et al. [44] measured the molecular area of these sterols in pure monolayers at air–water interface at a surface pressure of 12 mN/m and temperature at 22 °C and showed that 7DHC, ERGO and CHOL have similar molecular areas of 36.5 $Å^2$, 38.5 $Å^2$ and 39.0 $Å^2$, respectively. Serfis et al. [5] using the same method also showed that 7DHC monolayer collapsed at a molecular area of 34.5 $Å^2$ which is similar to CHOL (35.0 $Å^2$) at 37 °C. Therefore a significant difference in the spacing effect for these sterols in PC lipid bilayers is not expected.

With respect to the condensing effect, it has been suggested that a strong interaction of sterols with PC lipids depends on the availability of the smooth α face (the downside face showed in Fig. 1) [49]. As shown in Fig. 1, the CHOL molecule is flat and linear with all of its rings in a chair conformation lying in the same plane. As discussed earlier, 7DHC and ERGO have an extra double bond (C7–C8), and thus, exhibit a slight torsion or "puckering" of the rings. This "puckering" could prevent the 7DHC and ERGO from strongly interacting with surrounding DPPC or EggPC lipids in liposomes, and thus lead to a reduced condensing effect and a more negative zeta potential for 7DHC and ERGO incorporated liposomes. This is consistent with studies from Serfis et al. [5] in which EggPC-7DHC monolayers had a higher mean molecular area than obtained for EggPC-CHOL at same mole% of sterol and surface pressure. For example, at a surface pressure of 20 mN/m, Serfis and coworkers found that the mean molecular area for EggPC monolayers mixed with 10%, 20% and 30% of 7DHC were 80.7 $Å^2$, 70.2 $Å^2$ and 62.4 $Å^2$, respectively while the corresponding values were 76.2 $Å^2$, 66.5 $Å^2$ and 58.5 $Å^2$ when mixed with CHOL. Furthermore, from our work, it is clear that the difference in the structure of the side chain of ERGO and 7DHC has little effect on the zeta potential change of DPPC and EggPC liposomes. This suggests that structural change in the fused ring of the sterol is the more important factor in altering the local environment in the headgroup region of the liposomes.

While the zeta potential study provides information on the conformational order in the interfacial or headgroup region, the IR spectra data of CH_2 symmetric stretching bands at 2850 cm^{-1} provide information on the effects of sterol structure on the hydrocarbon chain conformational order. As shown in Fig. 6, addition of each of the three sterols in DPPC and EggPC membranes leads to a shift to a lower wavenumber for the CH_2 symmetric stretching band centered at 2850 cm^{-1}. This is consistent with other FTIR studies [20,25,50] and is reflective of an increase of the conformational order in the acyl chain region. It was also found that, in both DPPC and EggPC membranes, the decrease in the wavenumber of CH_2 symmetric stretching band is highest for CHOL than the other two sterols indicating a highest packing density of the tails with this sterol. This higher packing density of the tail leads to a smaller space between lipid headgroups than found for the insertion of other sterols resulting in a less of a decrease in the zeta potential for CHOL than for 7DHC and ERGO.

The difference in interactions for the three sterols with DPPC or EggPC lipid membrane is also reflected in changes of the IR band due to the carbonyl group at 1730 cm^{-1}. In particular, the value for the relative integrated intensity for the low-wavenumber component increased with incorporation of each of the three sterols in DPPC membrane whereas this value decreased in EggPC membrane (see Tables 1 and 2). This shows that incorporation of sterols leads to an increase in the level of hydration of the DPPC lipid bilayer and a decrease in hydration level for EggPC lipid bilayer at the region close to the carbonyl band. A similar trend for the relative integrated intensity of the low wavenumber component was observed by Arsov and Quaroni [20] for CHOL in DPPC and DMPC membranes going from below to above the phase transition temperature.

The wavenumber shift in the CH_2 band shows that incorporation of sterols induces a more tightly packed tail region in both DPPC

and EggPC films. The change in relative intensity of the C═O bands with incorporation of sterols shows a more hydrated headgroup region in DPPC films and less hydrated headgroup region in EggPC films. This supports the conclusions derived from the zeta potential measurements. In the DPPC membrane, incorporation of these sterols increases the degree of hydration by creating a space between lipid headgroups and exposing the C═O bond to more water, although a stronger hydrogen bonding to the OH group of sterols could also contribute to the change in relative intensity of the C═O bands. In contrast, EggPC in a fluid phase is already loosely packed with staggered headgroups protruding at various distances. In this case, the C═O groups are already exposed to water and the incorporation of sterols decreases the level of water interacting with the C═O groups. This is due to a larger condensing effect by the sterol insertion on the neighboring PC lipids than found with DPPC liposomes.

When comparing the effect of CHOL, 7DHC and ERGO insertion in DPPC from the shift in the C═O band, it is found that the incorporation of 7DHC and ERGO produces a higher level of hydration in the C═O region than CHOL and this is consistent with the data obtained from zeta potential measurements. A weaker interaction for 7DHC and ERGO with DPPC lipids leads to a more spacious headgroup region and higher level of hydration. A more spacious headgroup region with 7DHC and ERGO insertion than CHOL gives rise to a more negative zeta potential and more hydrogen bonded carbonyl groups.

For the EggPC membrane, examination of the shift in the C═O bands shows that 7DHC has a greater effect on reducing the degree of hydration of the C═O groups than CHOL and ERGO at a given sterol loading. This is in agreement with the detergent insolubility data. Incorporation of 7DHC in EggPC produces lipid domain while no detergent resistant domain was found for CHOL. The incorporation of 7DHC leads to a similar or even less packing density of the lipid tails in EggPC liposomes than CHOL (indicated by the shift in the CH_2 band at 2850 cm^{-1}). As discussed earlier, 7DHC preferably partitions in low unsaturated lipids in EggPC liposomes resulting in lipid domains while CHOL distributes more evenly in these lipids.

It is also noted that changes in the band position and shape of the two components of C═O bands show that conformational changes of the PC molecules occur with sterol insertion. For example, the incorporation of each of the three sterols in DPPC liposomes results in a shift to higher wavenumber along with a decrease in the band width for high wavenumber component of the C═O band and a shift to higher wavenumber with an increased band width for the low wavenumber component (see Table 1). This trend was observed for pure DPPC membranes undergoing phase transition from a gel phase to liquid-disordered phase [20]. This suggests that the presence of sterols leads to a more loosely packed headgroup region in the DPPC membrane when below the phase transition temperature and an increase of the membrane fluidity while the opposite trend for EggPC occurs (see Table 2) in that sterol insertion increases order in the EggPC membrane along with a decrease of the membrane fluidity. This conclusion is supported by a recent fluorescence anisotropy and NMR study that showed incorporation of cholesterol and other similar sterols leads to an increase of the fluidity and permeability of PC membranes in the gel phase (i.e., DPPC) and a decrease of the fluidity and permeability of those in fluid phase (i.e., POPC) [7].

5. Conclusions

Three methods (IR spectroscopy, detergent solubility and zeta potential measurements) have been used to study the effects of incorporation of CHOL, 7DHC and ERGO on the membrane structures of DPPC or EggPC liposomes. While the detergent insolubility measurements provided the information with lipid domain formation in PC liposomes containing varied amount of different sterols, zeta potential measurements provided information with conformational change in the headgroup of PC lipids in liposomes and the IR spectra gave information with the change in the packing of tails (using the CH_2 stretching band at 2850 cm^{-1}) and the degree of hydration (using the C═O band at 1730 cm^{-1}) in PC lipid membrane induced by the three sterols.

It is shown that both the ring structure and tail conformation in the three sterols contribute to the membrane structures of liposomes containing sterol and this effect is different in DPPC in gel phase and EggPC in fluid phase. An extra double bond in the fused ring of 7DHC prevents 7DHC from tightly packing with DPPC lipids and leads to less domain formation than CHOL whereas it clearly produces more lipid domain formation in EggPC. The zeta potential measurement and IR band of C═O at 1734 cm^{-1} show that such change in ERGO induces no difference from 7DHC in the conformation order in the interfacial and headgroup region of DPPC. The much stronger lipid domain formation for ERGO with DPPC might due to a stronger van der Waals interaction for its tail with the acyl chains of DPPC.

References

[1] J.K. Yamamoto, R.F. Borch, Photoconversion of 7-dehydrocholesterol to vitamin-D3 in synthetic phospholipid-bilayers, Biochemistry 24 (1985) 3338–3344.
[2] X.L. Xu, R. Bittman, G. Duportail, D. Heissler, C. Vilcheze, E. London, Effect of the structure of natural sterols and sphingolipids on the formation of ordered sphingolipid/sterol domains (rafts), J. Biol. Chem. 276 (2001) 33540–33546.
[3] C. Wolf, C. Chachaty, Compared effects of cholesterol and 7-dehydrocholesterol on sphingomyelin-glycerophospholipid bilayers studied by ESR, Biophys. Chem. 84 (2000) 269–279.
[4] C. Bernsdorff, R. Winter, Differential properties of the sterols cholesterol, ergosterol, beta-sitosterol, trans-7-dehydrocholesterol, stigmasterol and lanosterol on DPPC bilayer order, J. Phys. Chem. B 107 (2003) 10658–10664.
[5] A.B. Serfis, S. Brancato, S.J. Fliesler, Comparative behavior of sterols in phosphatidylcholine-sterol monolayer films, Biochim. Biophys. Acta - Biomembr. 1511 (2001) 341–348.
[6] Y.W. Hsueh, M.T. Chen, P.J. Patty, C. Code, J. Cheng, B.J. Frisken, M. Zuckermann, J. Thewalt, Ergosterol in POPC membranes: physical properties and comparison with structurally similar sterols, Biophys. J. 92 (2007) 1606–1615.
[7] A. Arora, H. Raghuraman, A. Chattopadhyay, Influence of cholesterol and ergosterol on membrane dynamics: a fluorescence approach, Biochem. Biophys. Res. Commun. 318 (2004) 920–926.
[8] M. Edidin, The state of lipid rafts: from model membranes to cells, Annu. Rev. Biophys. Biomol. Struct. 32 (2003) 257–283.
[9] X.L. Xu, E. London, The effect of sterol structure on membrane lipid domains reveals how cholesterol can induce lipid domain formation, Biochemistry 39 (2000) 843–849.
[10] G.S. Tint, M. Irons, E.R. Elias, A.K. Batta, R. Frieden, T.S. Chen, G. Salen, Defective cholesterol-biosynthesis associated with the Smith–Lemli–Opitz Syndrome, N. Engl. J. Med. 330 (1994) 107–113.
[11] T.N. Tulenko, K. Boeze-Battaglia, R.P. Mason, G.S. Tint, R.D. Steiner, W.E. Connor, E.F. Labelle, A membrane defect in the pathogenesis of the Smith–Lemli–Opitz syndrome, J. Lipid Res. 47 (2006) 134–143.
[12] R.K. Keller, T.P. Arnold, S.J. Fliesler, Formation of 7-dehydrocholesterol-containing membrane rafts in vitro and in vivo, with relevance to the Smith–Lemli–Opitz syndrome, J. Lipid Res. 45 (2004) 347–355.
[13] E.E. Berring, K. Borrenpohl, S.J. Fliesler, A.B. Serfis, A comparison of the behavior of cholesterol and selected derivatives in mixed sterol-phospholipid Langmuir monolayers: a fluorescence microscopy study, Chem. Phys. Lipids 136 (2005) 1–12.
[14] A.M. Smondyrev, M.L. Berkowitz, Molecular dynamics simulation of the structure of dimyristoylphosphatidylcholine bilayers with cholesterol, ergosterol, and lanosterol, Biophys. J. 80 (2001) 1649–1658.
[15] C. Chen, C.P. Tripp, An infrared spectroscopic based method to measure membrane permeance in liposomes, Biochim. Biophys. Acta - Biomembr. 1778 (2008) 2266–2272.
[16] J.W. Wang, Megha, E. London, Relationship between sterol/steroid structure and participation in ordered lipid domains (lipid rafts): implications for lipid raft structure and function, Biochemistry 43 (2004) 1010–1018.
[17] E. London, Insights into lipid raft structure and formation from experiments in model membranes, Curr. Opin. Struct. Biol. 12 (2002) 480–486.
[18] K. Makino, T. Yamada, M. Kimura, T. Oka, H. Ohshima, T. Kondo, Temperature-induced and ionic strength-induced conformational-changes in the lipid head group region of liposomes as suggested by zeta-potential data, Biophys. Chem. 41 (1991) 175–183.
[19] N. Deo, P. Somasundaran, Mechanism of mixed liposome solubilization in the presence of sodium dodecyl sulfate, Colloids Surf. A Physicochem. Eng. Aspects 186 (2001) 33–41.
[20] Z. Arsov, L. Quaroni, Direct interaction between cholesterol and phosphatidylcholines in hydrated membranes revealed by ATR-FTIR spectroscopy, Chem. Phys. Lipids 150 (2007) 35–48.
[21] M. Naumowicz, Z.A. Figaszewski, Impedance analysis of lipid domains in phosphatidylcholine bilayer membranes containing ergosterol, Biophys. J. 89 (2005) 3174–3182.

[22] R. Leventis, J.R. Silvius, Use of cyclodextrins to monitor transbilayer movement and differential lipid affinities of cholesterol, Biophys. J. 81 (2001) 2257–2267.
[23] W. Hubner, A. Blume, Interactions at the lipid–water interface, Chem. Phys. Lipids 96 (1998) 99–123.
[24] R. Lewis, R.N. McElhaney, W. Pohle, H.H. Mantsch, Components of the carbonyl stretching band in the infrared-spectra of hydrated 1,2-diacylglycerolipid bilayers — a reevaluation, Biophys. J. 67 (1994) 2367–2375.
[25] I. Fournier, J.B. Arwicz, M. Auger, P. Tancrede, The chain conformational order of ergosterol- or cholesterol-containing DPPC bilayers as modulated by Amphotericin B: a FTIR study, Chem. Phys. Lipids 151 (2008) 41–50.
[26] A. Csiszar, E. Koglin, R.J. Meier, E. Klumpp, The phase transition behavior of 1,2-dipalmitoyl-sn-glycero-3-phosphocholine (DPPC) model membrane influenced by 2,4-dichlorophenol-an FT-Raman Spectroscopy Study, Chem. Phys. Lipids 139 (2006) 115–124.
[27] T. Hianik, Structure and physical properties of biomembranes and model membranes, Acta Phys. Slovaca 56 (2006) 687–806.
[28] K.J. Seu, L.R. Cambrea, R.M. Everly, J.S. Hovis, Influence of lipid chemistry on membrane fluidity: tail and headgroup interactions, Biophys. J. 91 (2006) 3727–3735.
[29] J. Sabin, G. Prieto, J.M. Ruso, R. Hidalgo-Alvarez, F. Sarmiento, Size and stability of liposomes: a possible role of hydration and osmotic forces, Eur. Phys. J. E Soft Matter 20 (2006) 401–408.
[30] B. Biruss, C. Valenta, Comparative characterization of the physicochemical behavior and skin permeation of extruded DPPC liposomes modified by selected additives, J. Pharm. Sci. 96 (2007) 2171–2176.
[31] C.H. Huang, J.P. Sipe, S.T. Chow, R.B. Martin, Differential interaction of cholesterol with phosphatidylcholine on inner and outer surfaces of lipid bilayer vesicles, Proc. Natl. Acad. Sci. U. S. A. 71 (1974) 359–362.
[32] Y.K. Levine, M.H.F. Wilkins, Structure of oriented lipid bilayers, Nat. New Biol. 230 (1971) 69–72.
[33] H.I. Petrache, N. Gouliaev, S. Tristram-Nagle, R.T. Zhang, R.M. Suter, J.F. Nagle, Interbilayer interactions from high-resolution X-ray scattering, Phys. Rev. E 57 (1998) 7014–7024.
[34] J.F. Nagle, S. Tristram-Nagle, Structure of lipid bilayers, Biochim. Biophys. Acta - Rev. Biomembr. 1469 (2000) 159–195.
[35] W.J. Sun, R.M. Suter, M.A. Knewtson, C.R. Worthington, S. Tristram-Nagle, R. Zhang, J.F. Nagle, Order and disorder in fully hydrated unoriented bilayers of gel-phase dipalmitoylphosphatidylcholine, Phys. Rev. E 49 (1994) 4665.
[36] B. Cannon, G. Heath, J.Y. Huang, P. Somerharju, J.A. Virtanen, K.H. Cheng, Time-resolved fluorescence and Fourier transform infrared spectroscopic investigations of lateral packing defects and superlattice domains in compositionally uniform cholesterol/phosphatidylcholine bilayers, Biophys. J. 84 (2003) 3777–3791.
[37] E. London, D.A. Brown, Insolubility of lipids in Triton X-100: physical origin and relationship to sphingolipid/cholesterol membrane domains (rafts), Biochim. Biophys. Acta - Biomembr. 1508 (2000) 182–195.
[38] E. Endress, H. Heller, H. Casalta, M.F. Brown, T.M. Bayerl, Anisotropic motion and molecular dynamics of cholesterol, lanosterol, and ergosterol in lecithin bilayers studied by quasi-elastic neutron scattering, Biochemistry 41 (2002) 13078–13086.
[39] A. Kuksis, Yolk lipids, Biochim. Biophys. Acta 1124 (1992) 205–222.
[40] R. Silvius John, Role of cholesterol in lipid raft formation: lessons from lipid model systems, Biochim. Biophys. Acta - Biomembr. 1610 (2003) 174–183.
[41] Z. Cournia, G.M. Ullmann, J.C. Smith, Differential effects of cholesterol, ergosterol and lanosterol on a dipalmitoyl phosphatidylcholine membrane: a molecular dynamics simulation study, J. Phys. Chem. B 111 (2007) 1786–1801.
[42] T. Rog, M. Pasenkiewicz-Gierula, I. Vattulainen, M. Karttunen, Ordering effects of cholesterol and its analogues, Biochim. Biophys. Acta - Biomembr. 1788 (2009) 97–121.
[43] O. Edholm, J.F. Nagle, Areas of molecules in membranes consisting of mixtures, Biophys. J. 89 (2005) 1827–1832.
[44] R.A. Demel, K.R. Bruckdorfer, L.L.M. van Deenen, Structural requirements of sterols for the interaction with lecithin at the air–water interface, Biochim. Biophys. Acta - Biomembr. 255 (1972) 311–320.
[45] K. Kim, C. Kim, Y. Byun, Preparation of a dipalmitoylphosphatidylcholine/cholesterol Langmuir–Blodgett monolayer that suppresses protein adsorption, Langmuir 17 (2001) 5066–5070.
[46] E. Falck, M. Patra, M. Karttunen, M.T. Hyvoen, I. Vattulainen, Lessons of slicing membranes: interplay of packing, free area, and lateral diffusion in phospholipid/cholesterol bilayers, Biophys. J. 87 (2004) 1076–1091.
[47] S.W. Chiu, E. Jakobsson, R.J. Mashl, H.L. Scott, Cholesterol-induced modifications in lipid bilayers: a simulation study, Biophys. J. 83 (2002) 1842–1853.
[48] C. Hofsαβ, E. Lindahl, O. Edholm, Molecular dynamics simulations of phospholipid bilayers with cholesterol, Biophys. J. 84 (2003) 2192–2206.
[49] M.K. Jain, R.C. Wagner, Introduction to Biological Membranes, Wiley, New York, 1980.
[50] A. Dicko, T. Di Paolo, M. Pezolet, Interaction of dehydroepiandrosterone with phospholipid membranes: an infrared spectroscopy investigation, Biochim. Biophys. Acta - Biomembr. 1368 (1998) 321–328.